Chapter 73
How Do Fish Use the Movement of Other Fish to Make Decisions?

From Individual Movement to Collective Decision Making

Arianna Bottinelli, Andrea Perna, Ashley Ward, and David Sumpter

Abstract Recent experiments by Ward et al. have shown that fish a moving fish group detects hidden predators faster and more accurately than isolated individuals. The increase in speed, in particular, seems to be a consequence of the movement-mediated nature of the interactions used by fish to share information. The present work aims at investigating the link between movement and information transfer underlying collective decisions in fish. We define an individual-based self-propelled particle (SPP) model of the decision-making process analyzed by Ward et al. We fit it to data in order to deduce the smallest set of interaction rules consistent with the experimentally observed behaviour. We infer the relative weight of different social forces on fish movement during the decision-making process. We find that, in order to reproduce the observed experimental trends, both the social forces of alignment and attraction have to be introduced in the model, alignment playing a more important role than attraction. We finally apply this model to make theoretical predictions about fish ability to detect and avoid a moving predator in a natural environment such as open water.

Keywords Collective animal behaviour · Decision making · SPP models · Fish

73.1 Introduction

Animals living in groups are required to make collective decisions about where to collect food, the timing and direction of group travel, the choice of a new shelter or the detection and avoidance of predators [1]. The decision-making accuracy of groups is typically predicted to be greater than that of the single group members, initially increasing with group size before leveling off [2]. This phenomenon can be explained by the fact that larger groups of animals are more effective than smaller

A. Bottinelli (✉) · A. Perna · D. Sumpter
Uppsala University, Uppsala, Sweden

A. Ward
University of Sidney, Sidney, Australia

T. Gilbert et al. (eds.), *Proceedings of the European Conference on Complex Systems 2012*, Springer Proceedings in Complexity, DOI 10.1007/978-3-319-00395-5_73,

groups or solitary individuals at gathering information, whereas single group members can exploit the informations collected by other members of the group and integrate them to take better decisions [3]. The "many eyes" hypothesis, that ability to detect predators increases with group size, could be one of the main evolutionary drives for the formation of animal groups [4, 5].

While pooling information from different group members increases accuracy, this improvement may come at a cost in terms of decision speed. Under this scenario, the speed-accuracy trade-off would be due to the additional time spent by different individuals for pooling their individual preferences and converge to a unitary decision. Interestingly, however, in experiments the integration of informations possessed by different group members in a fish school was found not have a great cost in terms of speed, allowing not only for more accurate, but also for faster decisions [6]. While the increase in accuracy with group size is successfully predicted by a model of optimal information transfer among group members, the increase of speed seems to be a consequence of the specific nature of the interactions used by fish to share information. Interactions are encoded into fish response to their neighbours' behaviour and mediated by movement, allowing information to spread quickly through the group [7]. Subsequently, information is filtered and integrated according to some simple local heuristic rule [8, 9]. Understanding these heuristics, as well as the relevant cues related to fish movement that support information transfer, is an important step towards a comprehensive understanding of decision-making's experimental outcomes and, in general, towards a mechanistic-based explanation of group behaviour.

In the present work we aim at investigating the specific nature of movement interactions underlying fast and accurate collective decision in fish as observed in [6]. In order to describe fish motion and the decision making process together we took a modeling-numerical approach where fish are represented as interacting self-propelled particles (SPPs). These particles move in a two dimensional space by updating their position according to their own driving force (represented as vectors), but also according to social forces related to the motion of other fish. The whole ensemble of forces driving the particle's movement are called their "rules of motion", and the relative influence of different forces on the motion process is represented by the length of the corresponding vectors, these lengths being parameters of the model. We numerically reproduce the decision-making experiment analyzed by Ward et al. in [6] by setting the simulation in an environment that reproduces the experimental set-up. Our main goal here is to infer the relative importance of the different contributions to fish movement and, in particular, the relevance of social interactions during the collective choice of a group direction in order to escape an hidden predator.

Once obtained the relevant interactions and their relative importance, a further step in our work is to make theoretical predictions about their effectiveness in a different environment such as open water. We generalized the model in order to simulate groups of fish swimming according to the inferred rules of motion but free of the constraints of a tank and under the threat of a moving predator. Through a numerical approach we tested whether the same rules of motion could lead to

increases in the success of predator avoidance with group size also in this more general set-up.

73.2 Experimental Background: The Y-Maze Experiment

Our analysis is based on the empirical data collected by Ward et al. in [6]. In these experiments, the authors put groups of different size of mosquitofish, *Gambusia holbrooki*, in a Y shaped tank. A plastic model of a predator was allocated to one of the arms of the Y-maze at random and suspended in midwater to simulate a real predator. In pilot trials, the fish showed a strong aversive response to the predator once they detected it. During the experiment, five different group sizes of fish (1, 2, 4, 8, and 16) were added to a container set in the stem of the Y, then the box was raised, releasing the fish. In all cases, the fish made their way down the Y and into one of the arms. All trials were filmed and the fish were subsequently tracked.

Ward et al. were able to define two zones for their analysis: the area immediately before the bifurcation point of the tank, where the decision-making process takes place, called "decision zone" and the area crossed before reaching the decision zone, called "approach zone". The boundary between the two zones corresponded to the changing point in the behavior of the experimental animals before and during the decision-making process, and is situated around 16 cm from the bifurcation point of the Y-maze. For a picture of the experimental setup see Fig. 73.2.

In both the approach and the decision zones, each fish was characterized in terms of speed, path tortuosity (defined as the ratio of the path taken by the fish to the straight line distance between the beginning and the end of that path), time spent in the considered zone and the accuracy of its decision. The fish is considered to have made an accurate decision if enters into the arm of the Y-maze that does not contain the replica of the predator.

Ward et al. observed that, while a single fish is able to avoid the predator only in the 55.6 % of trials, which is not significantly different from random choice, the proportion of fish making an accurate decision increased with group size: individuals in groups of 8 or 16 fish were significantly more likely to make accurate decisions (i.e., to avoid the replica predator) than fish tested in isolation. The rate of increase in accuracy with group size was compatible with a perfect many eyes theory, stating that, for small groups of animals, the probability of all individuals avoiding the predator is equal to that of at least one individual detecting it. In particular, given the probability that a single fish spots the predator is p^1_{spot}, the probability that a group of size n avoids the predator is given by

$$P_n = 1 - \frac{1}{2}\left(1 - p^1_{spot}\right)^n \tag{73.1}$$

In [6], p^1_{spot} was computed from the one-fish experiment and resulted equal to 0.11 (under the assumption that when the fish fail to spot the predator they take a random branch of the Y-maze). The factor $1/2$ in Eq. (73.1) accounts for the fact

that even if the group does not spot the predator it has a 50 % chance of choosing the correct branch.

Ward et al. also measured that in the decision-making zone swimming speed is an increasing function of group size, while path tortuosity decreased with increasing group size. In particular, solitary fish and those in pairs decreased their swimming speed in the decision zone compared with the approach zone, whereas those in larger groups did not. This result is inconsistent with and expectation that integrating information among a larger number of individuals would require a longer time to converge to a collective decision.

73.3 Model and Methods

73.3.1 Fish as Interacting Self-Propelled Particles (SPPs)

One of the simplest ways of modeling animal movement and interaction is the Self-Propelled Particles approach introduced in 1995 by Vicsek and collaborators [10–13]. Animals are described as point particles moving with a constant speed and updating their direction at discrete time increments by adopting the average direction of motion of the particles in their local neighbourhood, plus a random perturbation [10]. This approach allows the study of the different global behaviours emerging from the introduction of different rules of interaction between particles (see [14] for a recent review), and therefore is particularly suited for our purpose of finding the minimal set of social interactions allowing for fast and accurate decisions.

Here, we consider the self-propelled particle model used in [15], and adapted from [16]. Each fish is a particle characterized by a direction of movement, a constant speed, an interaction radius R and a blind angle (see Fig. 73.1). At each time step, every fish will interact with all the neighbours within distance R, except for the ones in the region behind them, corresponding to the blind angle. The interaction radius together with the blind angle define an interaction zone whose size is equal for all the simulated fish and deduced from empirical data. We set the interaction radius to around 16 cm, which is also compatible with the size of the decision zone and the blind angle is fixed at 60 degrees from experimental considerations on the visual system of fish [17].

The direction of motion of each simulated fish is determined by the combined effect of different forces that act on the single particle. These contributions are described through vectors whose magnitude is proportional to their relative importance on the particle's motion, while the direction of the vectors can change at each time step, depending, for example, on the neighborhood of each fish. Forces contributing to the fish movement can be divided in two main subgroups: "individual forces" and "social forces". Individual forces represent basic characteristics of the fish movement, they are independent of the local neighborhood surrounding a particular fish, and describe its behaviour when it is alone. Conversely, social forces represent the tendency to align with or to join conspecifics within the local interaction zone of

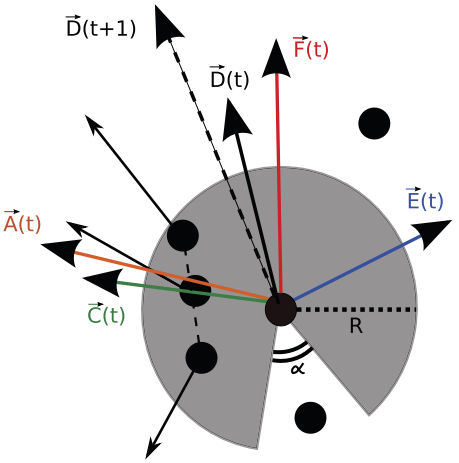

Fig. 73.1 Illustration of the SPP model. In the model fish are described as particles, each characterized by an interaction zone (*grey area* around the fish) defined by the interaction radius R and a blind angle α. While updating its position, the focal fish will take into account only the neighbours within this zone. The contributions to the movement of the fish are represented through forces acting on the particle (*arrows*), and we chose them to be the inertia in the current direction of movement $\vec{D}$, a force towards the favoured direction $\vec{F}$, an angular noise $\vec{E}$, the attraction towards the mass center of the interacting neighbours $\vec{C}$, and the alignment with their direction $\vec{A}$. The length of each vector represents the relative importance of the corresponding force, and is a parameter of the model. During simulations, at each time step all these contributions are computed and summed to give the new direction of movement of each fish $\vec{D}(t+1)$ (*dashed*)

each fish. As each fish experiences different interacting neighbourhood, these social forces are different for different individuals of the group.

The individual forces are inertia, aiming and a random force. The inertia $\vec{D}$ is the tendency to maintain the previous direction of motion. The "aiming force" $\vec{F}$ points towards the particles favoured direction. In the case of the y-shaped maze this point is the top shelter area of the maze. Then angular perturbation $\vec{E}$ represents uncertainty in the path. Lastly, at each time step the constant value of speed is perturbed by a Gaussian random error that is different for each fish and independent of neighbours. Note that this last addition does not introduce a further parameter since the value of speed is fixed according to the average speed measured from empirical data with the experimental standard deviation. These three forces together with the updating rule for speed are enough to describe the basic behaviour of a fish swimming alone [14].

Many options are available when it comes to introduce social forces, allowing to choose the level of detail in the description of individual behaviour [10–15]. Since our aim is to find the minimal set of interaction rules explaining experimental results, in the present model we introduce just two of them: the attraction towards the mass center of the interacting neighbours $\vec{C}$, and a force of alignment with their direction $\vec{A}$.

Given the above forces, the updating rule determining the actual motion of each fish is that at each time step all the described contributions are computed and summed to give the new direction of movement:

$$\vec{D}(t+1) = d\hat{D}(t) + f\hat{F}(t) + e\hat{E}(t) + c\hat{C}(t) + a\hat{A}(t) \tag{73.2}$$

Where all the forces have been decomposed in their modulus (small letter), which is the relevance of the force, as well as the unknown parameter of the model, and their unitary direction (capital, hatted letter). The resulting direction $\vec{D}(t+1)$ is then normalized, and each particle moves in the direction given by $\hat{D}(t+1)$ with speed taken from a Gaussian distributed around the mean experimental value.

73.3.2 Numerical Simulation of the Y-Maze Experiment

We simulated the decision-making process by running repeated simulations of groups of 1, 2, 4, 8 and 16 fish swimming in a Y-shaped environment of the same size of the experimental tank. Figure 73.2 shows the comparison between a typical run of the numerical simulations and a frame in an experimental trial with eight fish. In our simulated environment we distinguish three main zones, the approach zone, the decision zone and the zone after the bifurcation. The border between approach and decision zones is placed 16 cm from the bifurcation point, as in the experiments. At each run of the simulations the predator is randomly set in one of the two branches.

In a typical run of the simulation, the fish start from the beginning of the main branch of the Y maze, in the approach zone, with initial speeds, positions and entrance delays chosen according to experimental data. These delays are introduced to account for the fact that real fish do not all start moving through the maze at the same time. Since this is likely to have a consequence on the number of interacting neighbours per fish, we decided to reproduce such delays, as well as the other initial conditions, by randomly choosing a set of experimental initial conditions observed for a group of fish of the same size as the simulated one, and applying them to our simulations.

Once in the approach zone, fish move according to the rules of motions described in the previous section with, the force $\vec{F}$ pointing towards the top of the tank where the bifurcation is (see Fig. 73.2). This choice causes simulated fish to swim towards the decision zone and the branching point and reproduces the preference of real fish for deeper water and darker areas, as the two arms of the Y-shaped tank in experiments were [6].

The predator-avoidance task is numerically reproduced by assigning to each fish an individual probability $p^1_{spot} = 0.11$ of spotting the predator in the moment it enters in the decision zone. This probability is set according to experimental data so that on average a single fish has a final probability of 0.55 to avoid the predator, according to Eq. (73.1) [6]. In the case a fish spots the predator, it stops behaving according to the rules of motion and moves straight towards the safe branch

of the tank with the speed it had when entering the decision zone. Depending on the strength of the social forces compared to the individual ones, the influence of a spotting fish on its neighbours leads to different global outcomes, from the likely avoidance of the predator by the whole group in the case of strong social interactions, to the noninteracting case, in which the probability of avoiding the predator is 0.55 independent of the size of the group.

To fit the model, we ran repeated simulations of the decision-making process for a wide range of parameters' value, with the scale of interaction fixed to $d = 1$. The fitting procedure is divided in two steps: we first obtain the strength of the aiming direction f and of the noise e by matching data and simulations for one fish. We then used these values in simulations of larger groups (2, 4, 8, 16 fish) and compared them with the corresponding data sets to infer the values of the social forces of alignment a and attraction c.

In the first part of the fitting process we ran 108 numerical realizations of the decision-making process for one fish and for each couple (f, e) of the values representing the strength of the force towards the bifurcation point and of the angular noise. The number of realizations is the same number of experimental trials by Ward et al., and one realization is constituted of the average of 100 runs from the same randomly extracted initial condition. For each set of parameters and group size we computed two global observables in the decision zone, the path tortuosity described by Ward et al., and the circular standard deviation of fish turning. Circular standard deviation can be thought of as a measure of the entity of directional changes. It is given by

$$CStD(t) = \sqrt{-2\log\big(r(t)\big)}, \tag{73.3}$$

where, if $\theta_i(t)$ is the angular turning of the i-th fish at time t and N the group size, then

$$r(t) = \sqrt{\left(\frac{\sum \sin\theta_i(t)}{N}\right)^2 + \left(\frac{\sum \cos\theta_i(t)}{N}\right)^2}. \tag{73.4}$$

Once we obtained the average tortuosity (T) and circular standard deviation (CStD) for each couple of parameters (f, e), we selected only the values compatible with the empirical ones, i.e. the values that were within one standard deviation, and the corresponding sets of "good" parameters $(f, e)_T$ and $(f, e)_{CStD}$. We then chose the best values $(f, e)_{best}$ in the intersection of the above sets $(f, e)_\cap = (f, e)_T \cap (f, e)_{CStD}$ as the values for which the Euclidean distance between numerical and experimental observables was minimized:

$$(f, e)_{best} = \min_{(f,e)_\cap} \sqrt{(T_{sim} - T_{exp})^2 + (CStD_{sim} - CStD_{exp})^2}. \tag{73.5}$$

Note that the accuracy for a single fish was not calculated at this stage, since it was fixed by $p^1_{spot} = 0.11$.

In the second part of the fitting process, for each couple (a, c) of the values of the social forces we ran 16 numerical realizations for groups of 2, 4, 8 and 16 fish with the individual parameters $(f, e)_{best}$ inferred in the analysis described above.

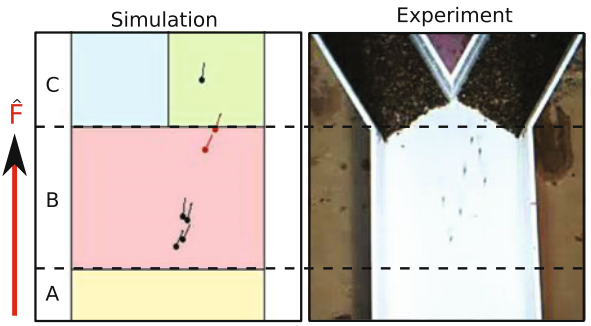

Fig. 73.2 Comparison between the visualization of our numerical set up and the experimental one. Following empirical results from [6], we distinguished three zones in our simulations: the approach zone (A), the decision zone (B) and the zone after bifurcation (C). Simulated fish started from the bottom of the tank, in the approach zone, with initial speeds, positions and entrance delays chosen according to experimental data. Fish swim across the tank due to the aiming force $\vec{F}$ that is set to point upwards, and have an individual probability $p^1_{spot} = 0.11$ of spotting the predator in the moment they enter the decision zone. This reproduces the experimental observed change in fish behaviour when crossing the threshold between zones A and B. The predator is randomly set in one of the two branches at the beginning of each run and a fish spotting it will stop behaving according to the rules of motion, swimming straight and with constant speed towards the safe branch

Again the number of numerical realizations is equal to the number of experimental trials in [6] and one realization is given by the average of 100 runs from the same randomly extracted initial condition. The process that allowed us to find the best values for alignment and attraction to neigbours follows a similar procedure as the one adopted to find the values of the individual forces. For each group size N, we computed the average accuracy (A) and tortuosity (T) and selected the couple of parameters $(a, c)^N$ corresponding to the values compatible with empirical results. We then intersected the couples of values obtained for tortuosity and accuracy $(a, c)^N_\cap = (a, c)^N_A \cap (a, c)^N_T$ at each group size, and subsequently took the union of these sets: $(a, c)_\cup = \cup_N (a, c)^N_\cap$. The best values $(a, c)_{best}$ are finally chosen from the union set $(a, c)_\cup$ as the values minimizing the Euclidean distance between experimental and numerical average for both accuracy and tortuosity:

$$(a, c)_{best} = \min_{(a,c)_\cup} \sqrt{\sum_N \left((A_{sim} - A_{exp})^2 + (T_{sim} - T_{exp})^2\right)_N}. \tag{73.6}$$

73.3.3 Simulations in Open Water

After fitting the parameters for the specific predator-avoidance task in the Y-maze, we adapted the model to numerically test the ability of the same fish to spot and escape a predator in different environmental conditions. Since the relevance of social interactions has been obtained for a very specific situation, we are interested

in whether the same rules of motion could lead to an increasing in the success of predator avoidance with group size also in a more general set-up. In particular, we simulate the model in open water for groups of shoaling fish of different size under the threat of a moving predator chasing them.

The first modification to the original model regards the set-up. Simulations take place in a squared tank centered in the axis origin and with a side that is one meter long. The predator is now free to move in the tank, and we now define some simple rules of motion. For the sake of simplicity, the only contributions to the predator's movement are inertia, which is set to be unitary, and a force of attraction towards the closest fish, which can be thought as the favourite direction of the predator. We chose this force to have the same strength as the aiming direction of fish $\vec{F}$ that we fitted from the Y-maze experiment. The speed of the predator is chosen to be constant and equal to 6 mm/frame, which is smaller than the lower average speed registered in experiments (that is, $v = 7.8$ mm/fr for one fish [6]). This choice, although arbitrary, is done in order to detect the advantage of the observed increasing in decision-making speed as a function of the group size. In the simulation, the predator starts from the upper-right corner of the tank, with an initial direction towards the origin of the axes.

The simulated fish are initially distributed with random positions and directions in a square of 10×10 centimeters, placed 30 centimeters away from the center of the tank. The initial speed of fish, as well as their speed throughout the whole simulations, is now extracted from the empirical distribution characterizing the corresponding group size in the Y-shaped tank experiment [6]. As regards the rules of motion of shoaling fish, the generalization of the model requires only a change in the favoured direction of the fish, i.e. in the direction of the aiming force $\vec{F}$, that in this set of simulations points towards the center of the tank. The effect of this choice is that the group will maintain a circular motion around the center of the tank without hitting the borders, preventing the definition of an interaction with walls.

In order to simulate the predator-avoidance task in open water, we assigned a spotting probability to each fish that is again $p^1_{spot} = 0.11$, but in this new environment a fish can spot the predator when their mutual distance is equal to the length of the decision zone. If this happens, the fish stops behaving according to the rules of motion, swimming straight and at a constant speed in the opposite direction with respect to the position of the predator, until it hits the walls of the tank. Once a fish reaches the border of the tank and exits it, it cannot go back and is considered to be "safe". As in the simulations of the Y-maze presented in the previous section, fish that do not detect the predator are influenced by the behaviour of the neighbours who did, and through social interactions has the chance to reach the border of the tank and avoid the predator. Conversely, a fish might not manage to escape the predator, whether it spots it or not, indeed if it gets closer than 6 cm from the point representing the predator[1] it is considered to be "eaten" and is canceled from simulations.

[1] This is chosen according to the fact that the predator replica used in [6] was 12 cm long.

In this setting, we ran 50 realizations for groups of fish of the same size as the ones analyzed in the Y-maze (1, 2, 4, 8 and 16), each realization being the average over 100 runs starting from the same initial condition and ending when all the fish are either "safe" or "eaten". For each group size we measured the proportion of fish avoiding the predator and the proportion of eaten fish. Among the "safe" fish, we then distinguished between these who avoided the predator because of detection and the ones escaping due to social interactions. Indeed, the latter quantity is the more relevant observable in order to assess the relevance of the social forces inferred in the Y-maze experiment in a predator-avoidance task.

73.4 Results

Initially we tried to describe fish as self-propelled particles interacting only by mean of attraction towards the mass center of neighbours, as in [16]. This was not sufficient to fit data. In fact, for each given group size the averaged observables assumed a value that was almost independent of the strength of attraction. Increasing with the value of the parameter c made little difference to the outcome, and even the best values did not compare favorably with experimental results. A similar situation was found when we tried to fit parameters by introducing only alignment with neighbours, as in [10]. Only the combination of these two social forces together provided significant variation in outcome as a function of parameters to allow us to successfully fit the data.

From the first step of the inference process, that is by matching the average simulated tortuosity and circular standard deviation with the corresponding experimental averages for one fish, we found the best values for the individual forces to be $(f, e)_{best} = (1.7, 2.7)$. Figure 73.3 shows the inference process leading to the obtained result. Here we plot the difference between the simulated observables (circular standard deviation and tortuosity respectively) and their empirical value for each couple (f, e) of the parameters. Both circular standard deviation and tortuosity increase with increasing angular noise and with decreasing aiming force, giving a regular surface whose difference with experimental values intersects zero in both cases. The black central band corresponds to the simulated quantities that are near to those found in experiments. The parameters (f, e) matching these values are reported in Fig. 73.3(C). This allows us to visualize the set $(f, e)_{\cap}$. This result is an intermediate step towards the fitting of social forces, but still it shows that randomness (e) is larger than the aiming force (f) and than inertia (d)

The second step was to look at simulations of groups of 2, 4, 8 and 16 fish. Varying the strength of social forces we finally fitted tortuosity and accuracy against data. Comparing simulated and experimental values at different values of the parameters (a, c) revealed that accuracy is an increasing function of both attraction and alignment. Tortuosity increases with attraction only, being a (slightly) decreasing function of alignment. Despite this trade-off between attraction and alignment in determining the trend of tortuosity, for all the group sizes it was possible to find

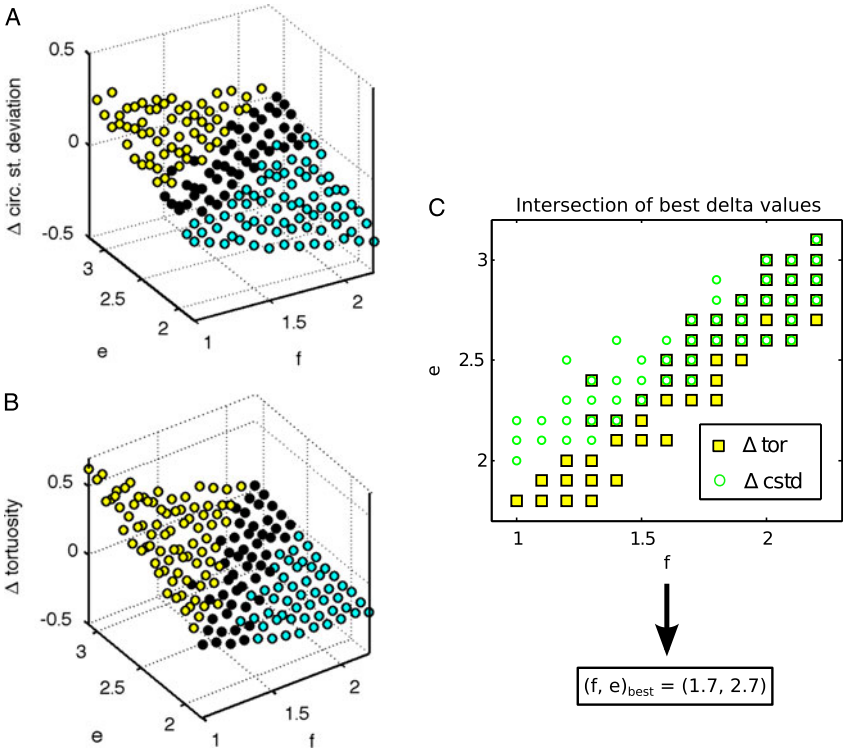

Fig. 73.3 Visualization of the inference process for the strength of individual forces. (**A**) and (**B**) The difference between the average of simulated observables (circular standard deviation and tortuosity respectively) for a single fish and their empirical value is plotted for each couple (f, e) of parameters. *The black central band* corresponds to the simulated quantities differing at most one standard deviation from the experimental values. (**C**) The couples of parameters (f, e) matching the black strip are reported in the same plane, square corresponding to the compatible values for tortuosity and circles for circular standard deviation. The couples of parameters corresponding to both a square and a circle constitute the set $(f, e)_{\cap}$, and a minimization on this intersection gave us $(f, e)_{best} = (1.7, 2.7)$

a set of parameters values for which simulations are compatible with empirical results. The final values of alignment and attraction resulting from the minimization process on the union of the compatible sets of parameters are $a = 4.2$ and $c = 3.1$. We do not show here the plots showing the variation of accuracy and tortuosity with the parameters (a, c), since they would not be particularly informative, and the visualization of the union set $(a, c)_{\cup}$ would be quite difficult due to the large number of subsets involved. Instead in Fig. 73.4 we show the match between our simulations and the data set from Ward's experiment. The simulations are in a good qualitative agreement with empirical data, reproducing quite closely the trends originally observed by Ward et al. These results suggest that alignment has a relevant role in the increasing of decision-making efficiency with group size. Notice that, despite circular standard deviation has been fitted to data only to retrieve the values of indi-

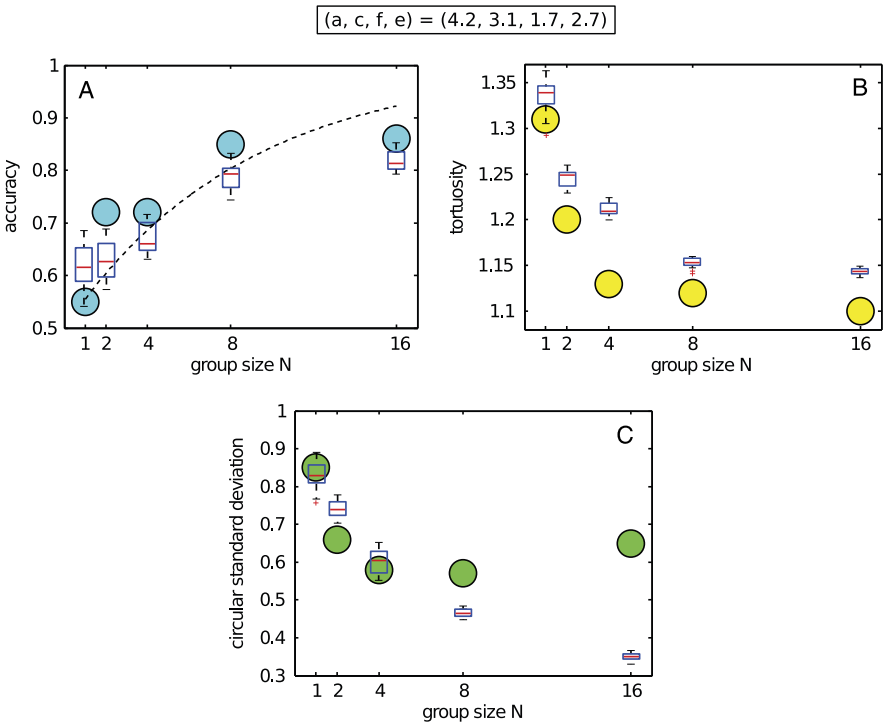

Fig. 73.4 Qualitative comparison between empirical data (*circles*) and numerical simulations (*boxes*). The model has been simulated with the parameters fixed to $(a, c, f, e) = (4.2, 3.1, 1.7, 2.7)$. Accuracy, tortuosity and circular standard deviation have been computed for each group size and plotted together with the corresponding experimental data. All the simulations are in a good qualitative agreement with empirical data, reproducing quite closely the trends originally observed by Ward et al. (**A**) Simulated accuracy is compatible with both empirical data and theoretical predictions at all group sizes. (**B**) Simulated tortuosity well resembles data for small group sizes, while at $N = 8$ and 16 decreasing is more difficult to achieve due to the trade-off between alignment and attraction in controlling this quantity. (**C**) Also the trend of circular standard deviation is reproduced, despite this observables has not been considered during the fitting of social interactions

vidual forces, the values of alignment and attraction obtained by fitting accuracy and tortuosity allow to also reproduce the trend of this third observable (Fig. 73.4(C)). Finally the robustness of the presented results have been tested by changing of the size of blind angle α from 0 to 180 degrees, showing no significant variation in the considered range.

We then tested the predator avoidance as a function of group size also in a more general set-up of open water. The test was performed by fixing the parameters according to the values obtained by fitting the Y-maze experiment, i.e. $(a, c, f, e) = (4.2, 3.1, 1.7, 2.7)$. The quantities that are relevant to assess the success in predator avoidance are the proportion of "safe" fish and the proportion of fish avoiding the predator due to social interaction only and not because they spot-

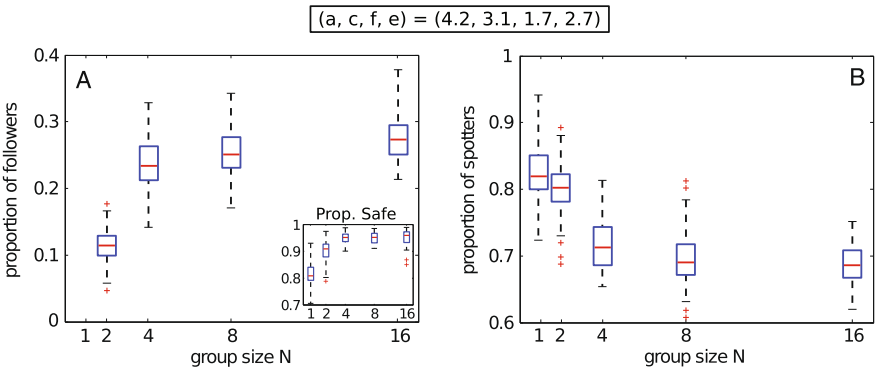

Fig. 73.5 Results of the simulations of the model in open water with $(a, c, f, e) = (4.2, 3.1, 1.7, 2.7)$. (**A**) The proportion of fish escaping due to social interactions only is an increasing function of group size, as well as the total proportion of safe fish (*inset*), meaning that the rules of motion fitted in the Y-maze make larger group more successful in predator avoidance also in different environment. (**B**) The proportion of spotting fish decreases with increasing group size, suggesting an important role of social interactions

ted it. The second quantity is particularly interesting, since it reveals how the actual relevance of social interactions relates with group size. In our simulations we found that both these observables are an increasing function of group size, (Fig. 73.5(A)), despite the surprising fact that the proportion of fish spotting the predator decreases with group size (Fig. 73.5(B)).

73.5 Conclusions

We have presented a first attempt to relate a collective decision-making process to the explicit rules of motion for fish movement. We have shown that a self-propelled particle model can reproduce the increasing speed and accuracy with group size. In doing so we inferred the explicit values of the parameters providing the best match to experimental data. Finally, we investigated the possibility of extending the obtained results to a more general setting by testing the fitted model in a different environment.

When defining the model we initially considered just one social force: the attraction towards the center of mass of the interacting neighbours. In a previous work on the same fish species (*Gambusia holbrooki*) as in the Ward et al. experiment, Herbert-Read et al. find only a weak role of alignment and a strong role for attraction while analyzing the rules of motion of groups of swimming in a square tank [18]. Furthermore, Strömbom has shown that a rich and complex range of behaviour can be achieved from only local attraction and a blind angle [16]. However, we found that it was not possible to fit data by mean of attraction alone. A similar situation was found when we tried to fit parameters by introducing only alignment. Only the combined contribution of these two social forces allowed us to fit the data.

It is therefore clear that fitting a basic self-propelled particle model requires both the social forces of alignment and attraction.

Not only is alignment important, but it is actually more important than attraction in information transfer mediating. This result is consistent with the suggestion that alignment with neighbors can allow information to be transmitted rapidly through fish schools [19]. At first sight, it appears however to be in contrast with experimental observations on the same fish [18]. There are however fundamental differences in the two analyzed settings. Herbert-Read and co-workers inferred the rules of motion for groups of mosquitofish swimming freely in a square tank after a period of acquaintance, where no decision making nor predation risk are involved. In such a circumstance it is reasonable to assume that the fish aim primarily to maintain cohesion. Attraction to conspecifics is then the most relevant force to achieve this goal by, for example, preserving a common speed. However, in a situation where fish have to collectively decide between the two arms of the tank, one of which is occupied by the predator replica, the goals of the fish change. Furthermore, the experimental set up adopted by Ward et al. does not allow fish to spread too much, already ensuring that the group will be quite packed. In this context, one explanation of the importance of alignment is that a sharp direction change provides a social cue about which of two available branches to take. A clear turning by the spotting fish communicates to conspecifics that it has some extra knowledge about which path to take, and the easiest way for other fish to be sure to take the safe branch of the tank is to assume its same direction. That is to align with the turning fish.

It is possible that our results and interpretation are strictly linked to the modeling choices we made in fitting data. The SPP approach introduces a strict distinction between forces and makes it necessary to choose which ones to introduce for representing interactions between fish. Our decision of prioritizing alignment and attraction over other social forces is arbitrary, and further work could be done by exploring if it would be possible to fit Ward's data by using different forces within an SPP model or even by trying different models. For example, introducing repulsion along with attraction instead of alignment could have lead to results more compatible with observations emphasizing the role of attraction [18]. Models have shown that highly polarized groups can be obtained from attraction and repulsion without involving alignment [16, 20]. Another alternative approach would be to fit different models than the ones involving social forces acting on self-propelled particles. Good candidates could be models where individual rules of motion are based on retinal information processing [21] or on simple heuristics integrating information about the surrounding environment [22]. Models involving speed variation, which appears to be an important feature characterizing fish motion [18, 23], could also provide a better fit. An interesting question in this direction is whether the rules of motion found by Herbert-Read and co-workers alone can explain the main features of the decision-making process observed by Ward et al. This could be investigated by defining a data-driven model based on the rules of motion found in [18], assigning a spotting probability to individual fish and simulating it in a Y-maze like environment. Despite the preliminary nature of the work presented here, it is the first attempt we know of to relate the empirical outcome of a collective decision-making

process to the explicit rules of motion of animals. There is much additional research which can be done in this area.

The last step in our work has been to ask about the possible generalizations of our model. By simulating the model in open water with the parameters fitted from the Y-maze experiment, we were able to observe that both the proportion of "safe" fish and the proportion of fish escaping the predator due to interactions are an increasing function of group size. These results support the hypothesis that the decision-making accuracy of groups is typically greater than that of the single group members [2]. Our analysis suggests that the interactions involved in the decision-making process in the Y-shaped tank should be the same social forces leading to a successful predator avoidance also in open water, and therefore they might turn out to be environment-independent.

A final intriguing hypothesis emerging from our analysis of the model in open water is that increased accuracy with group size may be accompanied with a decreased probability of individuals detecting predators. We found that the proportion of fish spotting the predator decreases with group size, while the proportion of safe fish increases. This result is consistent with an apparent decreased vigilance with group size. It is however inconsistent with the idea that it is "many eyes" which makes the group safer. It is rather fewer eyes and more efficient transfer of information that allows groups to outperform individuals.

References

1. Dall SRX, Giraldeau LA, Olsson O, McNamara JM, Stephens DW (2005) Information and its use by animals in evolutionary ecology. Trends Ecol Evol 20(4):187–193
2. King AJ, Cowlishaw G (2007) When to use social information: the advantage of large group size in individual decision making. Biol Lett 3(2):137–139
3. Couzin ID (2009) Collective cognition in animal groups. Trends Cogn Sci 13(1):36–43
4. Treherne J, Foster W (1980) The effects of group size on predator avoidance in a marine insect. Anim Behav 28(4):1119–1122
5. Lima SL (1995) Back to the basics of anti-predatory vigilance: the group-size effect. Anim Behav 49(1):11–20
6. Ward AJW, Herbert-Read JE, Sumpter DJT, Krause J (2011) Fast and accurate decisions through collective vigilance in fish shoals. Proc Natl Acad Sci USA 108(6):2312–2315
7. Sumpter D, Buhl J, Biro D, Couzin I (2008) Information transfer in moving animal groups. Theory Biosci 127(2):177–186
8. Sumpter DJT, Krause J, James R, Couzin ID, Ward AJW (2008) Consensus decision making by fish. Curr Biol 18(22):1773–1777
9. Ward AJW, Sumpter DJT, Couzin ID, Hart PJB, Krause J (2008) Quorum decision-making facilitates information transfer in fish shoals. Proc Natl Acad Sci USA 105(19):6948–6953
10. Vicsek T, András Czirók EBJ, Cohen I (1995) Novel type of phase transition in a system of self-driven particles. Phys Rev Lett 75:1226
11. Czirók A, Vicsek T (2000) Collective behavior of interacting self-propelled particles. Physica A 281:17–29
12. Czirok A, Barabasi A, Vicsek T (1999) Collective motion of self-propelled particles: kinetic phase transition in one dimension. Phys Rev Lett 82(1):209–212
13. Couzin ID, Krause J, James R, Ruxton GD, Franks NR (2002) Collective memory and spatial sorting in animal groups. J Theor Biol 218(1):1–11

14. Vicsek T, Zafeiris A (2012) Collective motion. Phys Rep. doi:10.1016/j.physrep.2012.03.004
15. Mann RP (2011) Bayesian inference for identifying interaction rules in moving animal groups. PLoS ONE 6(8):e22827
16. Strombom D (2011) Collective motion from local attraction. J Theor Biol 283(1):145–151
17. Rountree RA, Sedberry GR (2009) A theoretical model of shoaling behavior based on a consideration of patterns of overlap among the visual fields of individual members. Acta Ethol 12(2):61–70
18. Herbert-Read JE, Perna A, Mann RP, Schaerf TM, Sumpter DJT, Ward AJW (2011) Inferring the rules of interaction of shoaling fish. Proc Natl Acad Sci USA 108(46):18726–18731
19. Radakov D (1973) Schooling in the ecology of fish. Wiley, New York
20. Romey WL (1996) Individual differences make a difference in the trajectories of simulated schools of fish. Ecol Model 92(1):65–77
21. Lemasson B, Anderson J, Goodwin R (2009) Collective motion in animal groups from a neurobiological perspective: the adaptive benefits of dynamic sensory loads and selective attention. J Theor Biol 261(4):501–510
22. Moussaïd M, Guillot EG, Moreau M, Fehrenbach J, Chabiron O, Lemercier S, Pettré J, Appert-Rolland C, Degond P, Theraulaz G (2012) Traffic instabilities in self-organized pedestrian crowds. PLoS Comput Biol 8(3):e1002442
23. Hemelrijk CK, Hildenbrandt H, Reinders J, Stamhuis EJ (2010) Emergence of oblong school shape: models and empirical data of fish. Ethology 116(11):1099–1112